DoA Estimation via Unlimited Sensing

Samuel Fernández-Menduiña*, Felix Krahmer†, Geert Leus‡ and Ayush Bhandari*
* Dept. of Electronic and Electrical Engineering, Imperial College London, SW72AZ, UK.
†Dept. of Mathematics, Technical University of Munich, Garching 85747, Germany.
‡Dept. of Microelectronics, Fac. EEMCS, Technical University of Delft, Mekelweg 4, 2628 CD Delft.
Email: *sf219@ic.ac.uk, †felix.krahmer@tum.de, ‡g.j.t.leus@tudelft.nl, *a.bhandari@imperial.ac.uk

***Abstract*—Direction-of-arrival (DoA) estimation is a mature topic with decades of history. Despite the progress in the field, very few papers have looked at the problem of DoA estimation with unknown dynamic range. Consider the case of space exploration or near-field and far-field emitters. In such settings, the amplitude of the impinging wavefront can be much higher than the maximum recordable range of the sensor, resulting in information loss via clipping or sensor saturation. In this paper, we present a novel sensing approach for DoA estimation that exploits hardware-software co-design and is pivoted around the theme of unlimited sensing. On the hardware front, we capitalize on a radically new breed of analog-to-digital converters (ADCs) which, instead of saturating, produce modulo measurements. On the algorithmic front, we develop a mathematically guaranteed DoA estimation technique which is non-iterative and backwards compatible with existing DoA algorithms. Our computer experiments show the efficiency of our approach by estimating DoAs from signals which are orders of magnitude higher than the ADC threshold. Hence, our work paves a new path for inverse problems linked with DoA estimation and at the same time provides guidelines for new hardware development.**

***Index Terms*—Direction of arrival (DoA) estimation, multi-channel, non-linear sensing, sensor arrays, sampling theory.**

I. Introduction

The art of using multiple sensors for spatio-temporal acquisition of information has several decades of history. One of the core applications of sensor arrays is direction-of-arrival (DoA) estimation which dates back to the pioneering work of Marconi in the beginning of the 20^{th} century [1]. While DoA estimation is a mature topic [2], the advent of new hardware and applications continually pushes the envelope of the DoA algorithmic machinery. In the last many years, research efforts have been mainly focused towards exploring new array geometries [3]–[5] and designing algorithms for high resolution DoA estimation [6], [7].

DoA Estimation and Dynamic Range Problem. Our work is concerned with a different class of DoA estimation problems, where the amplitude range of the impinging signal is unknown and possibly much larger than the maximum recordable voltage of the analog-to-digital converter (ADC). This problem arises from practical contexts. We list two examples below.

- In space explorations, scientific equipment in the probe employs sensor arrays for various tasks such as source localization and sub-surface mapping. In foreign environments, for instance radar systems on lunar surfaces [11], the range of signal amplitudes is unknown and automatic gain control (AGC) is employed either during capture or in post-processing. NASA's Apollo Mission report [12] elaborates on the omnipresent use of AGCs and reports the sensor saturation problem (cf. pg 43, [12]). Even if the ADCs (equipped with AGCs) are calibrated, bursts and spikes [13] can saturate the sensor array, resulting in clipped measurements. This typically happens in the case of radars and seismic systems.
- A more familiar example of sensor array saturation stems from the *near-far* problem. Suppose that only two emitters are considered, and one of them is much closer to the receiver than the other. Then, the ADC can either focus on the near-field emitter, drowning the far-field emitter in quantization noise, or aim at retrieving the information of the far-field emitter, clipping the samples of the near-field emitter [14].

Beyond the problems listed above, the general trend in the recent years has been to use ADCs which can work with *wideband* receivers. It is well established that wideband ADCs require higher dynamic range [15], [16]. Surprisingly,

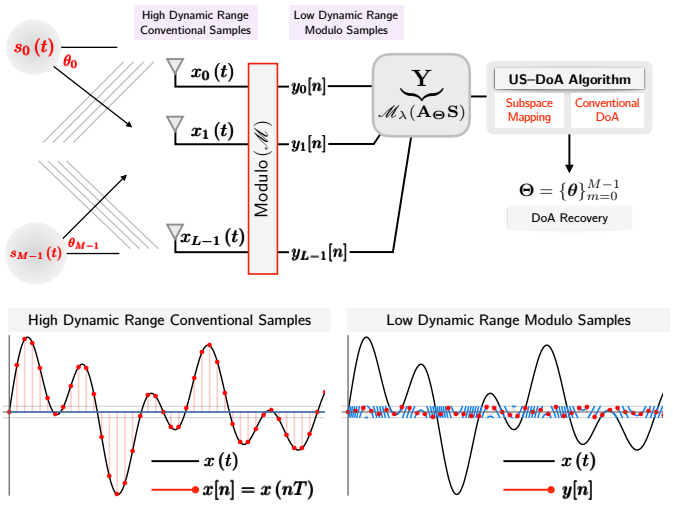

Fig. 1: Direction of arrival estimation using unlimited sensing architecture [8]–[10]. Modulo non-linearity maps high-dynamic-range, *sensor array* samples into low-dynamic-range *folded* samples. While the modulo operation prevents the sensor saturation problem, it leads to a new form of information loss which can be handled by capitalizing on the idea of unlimited sampling.

This work is supported by the UK Research and Innovation council's FLF program *Sensing Beyond Barriers* (award no. MR/S034897/1) and the *European Partners Fund 2019* (award no. G38037).

despite the significant advancements in DoA estimation, very few papers pose the problem with dynamic range constraints. To this end, a notable example is the work of Bar-Shalom and Weiss [17] who present the idea of one-bit ADC based DoA estimation. This approach circumvents the problem of clipping and even using AGCs. However, the one-bit mode of operation is at the other end of the spectrum of solutions —entire signal information is lost and only DoAs can be estimated. While this low-complexity solution is aptly justified for wireless communications, in many applications it is of interest to recover the signal itself. For example, in space exploration, experiments entail exorbitant costs and are non-repeatable. Similarly, in bio-medical [18] and ultrasound [19] applications, the signal itself encodes important information.

Solution via Modulo Non-Linearity. In what follows, we will present a new approach to the DoA estimation problem based on *co-design* of hardware and algorithms. Our work capitalizes on the recent developments around *unlimited sensing* [8]–[10]. Instead of working with conventional, point-wise samples of a function, which may be clipped, we opt to use folded amplitudes in the interval $[-\lambda, \lambda]$, where $\lambda > 0$ is the maximum recordable voltage of the ADC. On the hardware side, injecting modulo non-linearity in the sensing process results in folded measurements, as shown in Fig. 1. Mathematically, this can be written in terms of the following operator,

$$\mathscr{F}_\lambda : t \mapsto 2\lambda \left(\left[\!\left[\frac{t}{2\lambda} + \frac{1}{2} \right]\!\right] - \frac{1}{2} \right), \tag{1}$$

where $\mathscr{F}_\lambda(\cdot)$ is the conventional, centered modulo operation, and $[\![t]\!] \doteq t - \lfloor t \rfloor$ denotes the fractional part of t. Hence, arbitrarily high amplitudes beyond the dynamic range of the ADC are folded back into the recordable range $[-\lambda, \lambda]$ (cf. Fig. 1). Thanks to the recent, radical advances in ADC design technology, such non-linearities can be implemented via folding or self-reset ADCs [20], [21]. For further discussion on the link between folding ADCs and modulo non-linearities, we refer the readers to [9]. Even when the problem of recovering measurements from modulo samples is highly ill-posed, a sampling theorem and algorithm applicable to bandlimited functions have been already proposed in [8], [9]. The main result is as follows,

Theorem 1 (Unlimited Sampling Theorem [8])**.** *Let $x(t)$ be a continuous-time, finite-energy, bandlimited function with maximum frequency Ω and let $y[n] = \mathscr{F}_\lambda(x(nT))$ be its modulo samples with sampling rate T. Then, a sufficient condition for recovery of $x(t)$ from its modulo samples (up to an additive multiple of 2λ) is $T \leqslant 1/2\Omega e$.*

Remarkably, this sampling theorem does not depend on λ and depends *only* on the signal bandwidth; just like Shannon's sampling theorem. For a detailed discussion on the sampling theorem and associated algorithm, we refer the reader to [9].

A. Contributions

- We take a first step towards the formalization of the DoA estimation problem based on low-dynamic-range, modulo samples $y[n] = \mathscr{F}_\lambda(x(nT))$.
- We provide a simple recovery algorithm that is backwards compatible with known DoA estimation and beamforming methods. The recovery guarantees are agnostic to λ.

B. Advantages of DoA Estimation with Modulo Samples

Compatibility with Known DoA Estimation Techniques. An appealing feature of our method is its simplicity. Although our approach starts with non-linear, modulo samples $y[n]$, we show that existing DoA methods can be applied on a transformed version of $y[n]$, that is, $\mathcal{T}(y[n])$. As it will be shown, $\mathcal{T}(y) = \mathscr{F}_\lambda(\Delta^K y)$ is a point-wise, single-shot mapping, where Δ^K is the finite difference operator of order K. With $\mathcal{T}$, DoA estimation is mathematically guaranteed to succeed provided that we choose (T, K) according to the unlimited sampling theorem (cf. Theorem 1 and [9]).

Reduction in Computational Complexity What distinguishes this paper from our preceding works [8], [22], [23] is that here, (a) we are working with multi-channel measurements and (b) DoAs can be directly estimated from the modulo samples; there is no need to reconstruct the signal. This results in a *reduction* of both the computational requirements and the sampling density.

Compatibility with Beamforming. Compared to 1-bit encoding methods, a distinct advantage of our approach is that we can perform beamforming. In fact, we can perform beamforming directly on $\mathcal{T}(y[n])$, since Δ^K does not affect the space-dimension of the data. Such invariance allows retrieving only the unfolded samples from the desired sources instead of repeating the whole process on each antenna individually, which further reduces the complexity.

II. Problem Setup

Notation. Continuous functions and discrete sequences are represented by $x(t), t \in \mathbb{R}$ and $x[n], n \in \mathbb{Z}$, respectively. Matrices and vectors are written in capital and small, boldface font, respectively. For a matrix $\mathbf{X}$, we define $[\mathbf{X}]_{m,n}$ as the entry in the position (m, n) where we start counting from zero. We use $\mathbf{X}^{\mathsf{H}}$ and $\mathbf{X}^{\top}$ to denote conjugate-transpose and transpose of matrix $\mathbf{X}$, respectively. The covariance of a matrix $\mathbf{X}$ is written as $\mathcal{R}(\mathbf{X}) = \mathbf{X}\mathbf{X}^{\mathsf{H}}$. We use $\ker(\mathbf{X})$ and $\operatorname{span}(\mathbf{X})$ to denote the kernel and span of a matrix, respectively. Function and sequence spaces are denoted by $\mathbf{L}_p$ and $\boldsymbol{\ell}_p$, respectively and the corresponding norms are defined by $\|\cdot\|_{\mathbf{L}_p(\mathbb{R})}$ and $\|\cdot\|_{\boldsymbol{\ell}_p(\mathbb{R})}$. When $p \to \infty$, the norms denote the max-norm. A function x bandlimited to maximum frequency Ω is denoted by $x \in \mathcal{B}_\Omega$ while $x \in \mathsf{PW}_\Omega$ denotes a function in the Paley–Wiener class of bandlimited and square-integrable functions, $x \in \mathcal{B}_\Omega \cap \mathbf{L}_2$.

A. Data Model

We consider the standard setup in sensor array processing [1]. Suppose that M narrow band sources $\{s_m(t)\}_{m=0}^{M-1}$ with DOAs $\boldsymbol{\Theta} = \{\theta_m\}_{m=0}^{M-1}$, impinge on a uniform linear array

(ULA) with L sensors. The resulting data model for the l^{th} sensor ($l = 0, \ldots, L-1$) is written as,

$$x_l[n] = \sum_{m=0}^{M-1} a_l(\theta_m)\, s_m[n] \tag{2}$$

where,

- $x_l[n] = x_l(nT)$, $n = 0, 1, \ldots, N-1$, is the sampled waveform corresponding to the l^{th} sensor, which can be stacked in the matrix $\mathbf{X}$ as $[\mathbf{X}]_{l,n} = x_l[n]$.
- $a_l(\theta_m)$ is the l^{th} entry of the array steering vector given by,

$$\mathbf{a}(\theta_m) = \begin{bmatrix} 1 & e^{\jmath d \frac{\omega}{c} \sin(\theta_m)} & \cdots & e^{\jmath d \frac{\omega}{c}(L-1)\sin(\theta_m)} \end{bmatrix}^\top$$

  where the θ_m's are all distinct. The resulting matrix is,

$$\mathbf{A}_{\boldsymbol{\Theta}} = \begin{bmatrix} \mathbf{a}(\theta_0) & \cdots & \mathbf{a}(\theta_{M-1}) \end{bmatrix}. \tag{3}$$

- $s_m[n] = s_m(nT)$, $n = 0, \ldots, N-1$, are the samples of the m^{th} narrowband waveform, which can be stacked in the matrix $\mathbf{S}$ as $[\mathbf{S}]_{m,n} = s_m[n]$. Here, we will assume that $s_m \in \mathsf{PW}_\Omega$ (Paley-Wiener class), and hence $T \leqslant \pi/\Omega$ according to Shannon's sampling theorem.

In a compact form, given M sources, L sensors and N time-samples, the relationship between the matrices $\mathbf{X}$, $\mathbf{A}_{\boldsymbol{\Theta}}$ and $\mathbf{S}$ is given by,

$$\underbrace{\mathbf{X}}_{\mathbb{C}^{L\times N}} = \underbrace{\mathbf{A}_{\boldsymbol{\Theta}}}_{\mathbb{C}^{L\times M}} \underbrace{\mathbf{S}}_{\mathbb{C}^{M\times N}}. \tag{4}$$

In our work, we aim to recover the unknown DOAs $\boldsymbol{\Theta}$ from modulo measurements. Since the entries of the folding operation are complex–valued, the modulo operator $\mathscr{M}_\lambda(\cdot)$ should be interpreted in the following sense,

$$\mathscr{M}_\lambda(t) : t \in \mathbb{C} \to \mathscr{F}_\lambda(\Re(t)) + \jmath \mathscr{F}_\lambda(\Im(t)), \tag{5}$$

The DOA estimation problem boils down to recovering $\boldsymbol{\Theta}$ from point-wise non-linear measurements,

$$\mathbf{Y} \doteq \mathscr{M}_\lambda(\mathbf{X}) = \mathscr{M}_\lambda(\mathbf{A}_{\boldsymbol{\Theta}}\mathbf{S}). \tag{6}$$

The definition of the folding operator $\mathscr{M}_\lambda$ in (5) allows us to map $\mathbf{X} \in \mathbb{C}^{L\times N}$ to $\mathbf{Y} \in \mathbb{C}^{L\times N}$. A graphical representation of the setup is shown in Fig. 1.

B. Geometry of the DoA Estimation Problem

Existing techniques for DoA estimation cannot be directly applied in this scenario. To give the reader an intuitive understanding, consider the geometry of the eigen-decomposition and the rank constraint on $\mathcal{R}(\mathbf{X})$; the covariance matrix of the conventional data samples. It is well known that the eigen-decomposition of $\mathcal{R}(\mathbf{X})$ takes the form of,

$$\mathcal{R}(\mathbf{X}) = \mathbf{A}_{\boldsymbol{\Theta}} \mathcal{R}(\mathbf{S}) \mathbf{A}_{\boldsymbol{\Theta}}^{\mathsf{H}} = \mathbf{U}\boldsymbol{\Lambda}\mathbf{U}^{\mathsf{H}}. \tag{7}$$

The diagonal matrix $\boldsymbol{\Lambda}$ is at most rank M (in the absence of noise). This property is lost when working with data matrix $\mathbf{Y}$. To see this, let us recall the *Modulo Decomposition Property* [9] which allows to write $x(t) = \mathscr{M}_\lambda(x(t)) + \mathscr{Q}_x^\lambda(t)$ where $\mathscr{Q}_x^\lambda \in 2\lambda\mathbb{Z}$ is a simple function. In the context of our work, modulo decomposition implies that the data matrix can be decomposed as $\mathbf{X} = \mathbf{Y} + \mathscr{Q}_{\mathbf{X}}^\lambda$, and hence,

$$\mathcal{R}(\mathbf{Y}) = \mathcal{R}(\mathbf{X}) + \underbrace{\left(\mathcal{R}\left(\mathscr{Q}_{\mathbf{X}}^\lambda\right) - \left(\mathbf{X}\mathscr{Q}_{\mathbf{X}}^{\lambda,\mathsf{H}} + \mathscr{Q}_{\mathbf{X}}^\lambda \mathbf{X}^{\mathsf{H}}\right)\right)}_{\text{Noise}}. \tag{8}$$

Consequently, $\mathcal{R}(\mathbf{Y})$ can be interpreted as a noisy version of $\mathcal{R}(\mathbf{X})$ in (7). Therefore, standard techniques can not be applied unless a denoising strategy is employed.

III. DoA Estimation from Modulo Samples

A. Intuition and Overview of the Approach

In this work, starting with sampled data matrix $\mathbf{Y}$, we apply a transformation $\mathcal{T}$ such that $\mathbf{Z} = \mathcal{T}(\mathbf{Y})$ maps to the original signal subspace $\mathbf{X}$ but *not necessarily* to $\mathbf{X}$ itself. Once this is possible, we can use existing DoA estimation methods. Our approach leverages the idea that higher order differences taken over the samples (denoted by Δ^K) and the modulo operator $\mathscr{M}_\lambda(\cdot)$ commute in a certain sense [9]. For a smooth sequence, $x[n] = x(nT)$, the application of Δ^K has a shrinking effect on the derivative of the same function which is controlled by T^K. Hence, for a certain choice of sampling rate T and difference order K, it is possible to shrink the amplitudes of a sequence arbitrarily. Once the difference sequence is smaller than λ, the folding operation in (6) has no effect. This is because for any $\|a\|_{\boldsymbol{\ell}_\infty(\mathbb{R})} \leqslant \lambda$, we have that $a[n] = \mathscr{M}_\lambda(a[n])$. The net effect is that folding has no impact on the higher order differences and hence, starting with modulo measurements, we can access the higher order differences of the original sequence using $\mathcal{T}(\mathbf{Y}) = \mathscr{M}_\lambda\left(\Delta^K(\mathbf{Y})\right)$. Now, since differences are linear operators, their action on the subspace of bandlimited functions preserves the subspace structure.

B. Recovery Guarantees

Formally, let $x^{(K)}(t)$ denote the K^{th} order derivative of $x(t)$ and $\left(\Delta^K x\right)[n]$ be the finite difference of the sequence $x[n]$, with $(\Delta x)[n] = x[n+1] - x[n]$. The following lemma gives a relation between $\Delta^K x$ and $x^{(K)}$ in terms of the max–norm.

Lemma 1 (Difference-Derivative Inequality [8], [9])**.** *For any $x(t) \in \mathbf{C}^K(\mathbb{R}) \cap \mathbf{L}_\infty(\mathbb{R})$, its samples $x[n] \doteq x(nT)$ satisfy,*

$$\|\Delta^K x\|_{\boldsymbol{\ell}_\infty(\mathbb{R})} \leqslant (Te)^K \|x^{(K)}\|_{\mathbf{L}_\infty(\mathbb{R})}. \tag{9}$$

Using $T < 1/e$ allows us to shrink the amplitudes on the right hand side of (14). Typically, it is much easier to estimate the maximum value of the function than a bound on its derivative. To bound the right hand side of (9), we invoke the well known Bernšteĭn's inequality for bandlimited functions; for all $x \in \mathcal{B}_\Omega$, we have, $\|x^{(K)}\|_{\mathbf{L}_\infty(\mathbb{R})} \leqslant \Omega^K \|x\|_{\mathbf{L}_\infty(\mathbb{R})}$. By combining this with (9), we obtain the following bound in [9],

$$\|\Delta^K x\|_{\boldsymbol{\ell}_\infty(\mathbb{R})} \leqslant (T\Omega e)^K \|x\|_{\mathbf{L}_\infty(\mathbb{R})}. \tag{10}$$

Let $\mathcal{B}_x > \lambda$ be a known upper bound on $x(t)$. Choosing $T\Omega e < 1$ in (10) ensures $(T\Omega e)^K \mathcal{B}_x \leqslant \lambda$, for K given by

$$K \geq \left\lceil \frac{\log\lambda - \log\mathcal{B}_x}{\log(T\Omega e)} \right\rceil, \tag{11}$$

which is independent of M. Thus, letting $T < 1/\Omega e$,

$$\|\Delta^K x\|_{\boldsymbol{\ell}_\infty(\mathbb{R})} \leqslant \lambda \Rightarrow \Delta^K x = \mathscr{M}_\lambda\left(\Delta^K x\right). \tag{12}$$

To relate higher order differences of x with the measurements y, we use the following proposition [9],

Proposition 1. *For any sequence $x[n]$ it holds that*

$$\mathscr{M}_\lambda\left(\Delta^K x\right) = \mathscr{M}_\lambda\left(\Delta^K\left(\mathscr{M}_\lambda(x)\right)\right). \tag{13}$$

In our setup, since the time-domain samples are arranged along the row-dimension of $L \times N$ matrix $[\mathbf{X}]_{l,n} = x_l(nT)$, the difference operator acts over each row independently,

$$[\Delta^K \mathbf{X}]_{l,n} = \left(\Delta^K x_l\right)(nT) = [\mathbf{X}\mathbf{D}_K]_{l,n} \tag{14}$$

where $\mathbf{D}_K \in \mathbb{R}^{N\times(N-K)}$ is the matrix corresponding to Δ^K and $\mathbf{D}_0 = \mathbf{I}$ (identity matrix). Combining (13) and (12), we obtain the link between higher order differences and the modulo samples,

$$\Delta^K x = \mathscr{M}_\lambda\left(\Delta^K y\right) \overset{(14)}{\longleftrightarrow} \mathbf{X}\mathbf{D}_K = \mathscr{M}_\lambda\left(\mathbf{Y}\mathbf{D}_K\right). \tag{15}$$

We summarize our main result in the following theorem.

Theorem 2 (US–DoA)**.** *Let $\{s_m\}_{m=0}^{M-1} \in \mathcal{B}_\Omega$ be M, bandlimited functions and $s_m[n] = s_m(nT)$, $n = 0, \ldots, N-1$, be the samples with sampling rate T. Furthermore, let the modulo samples be stacked in the data matrix $\mathbf{Y} = \mathscr{M}_\lambda(\mathbf{A}_{\boldsymbol{\Theta}}\mathbf{S})$ in* (6) *with $\mathbf{A}_{\boldsymbol{\Theta}}$ defined in* (3)*. Provided that the sampling rate satisfies the sampling bound, $T \leqslant 1/2\Omega e$ and for some $N > K$, choosing,*

$$\mathcal{B}_x \geqslant \max_{0\leqslant l\leqslant L-1} \|x_l\|_{\mathbf{L}_\infty(\mathbb{R})} \text{ and } K \geq \left\lceil \frac{\log\lambda - \log\mathcal{B}_x}{\log(T\Omega e)} \right\rceil$$

results in (15)*, $\mathbf{X}\mathbf{D}_K = \mathscr{M}_\lambda(\mathbf{Y}\mathbf{D}_K)$.*

Instead of recovering $\mathbf{X}$ from $\mathbf{X}\mathbf{D}_K$ (higher order differences), which was the case in previous works on the topic of unlimited sampling [8], [22], [23], here we are interested in estimating DoAs. To this end, let us denote,

$$\mathbf{Z} \doteq \mathscr{M}_\lambda\left(\mathbf{Y}\mathbf{D}_K\right) = \mathbf{X}\mathbf{D}_K. \tag{16}$$

Accordingly, we obtain the eigenvalue decomposition of the covariance matrix, $\mathcal{R}(\mathbf{Z}) = \mathbf{U}\boldsymbol{\Lambda}\mathbf{U}^{\mathsf{H}} \equiv \mathbf{A}_{\boldsymbol{\Theta}}\mathcal{R}\left(\overline{\mathbf{S}}\right)\mathbf{A}_{\boldsymbol{\Theta}}^{\mathsf{H}}$, where $\overline{\mathbf{S}} = \mathbf{S}\mathbf{D}_K$. This shows that the operator Δ^K preserves the array manifold. For subspace based techniques, such as MUSIC or ESPRIT the following result has to be considered.

Proposition 2. *Let $\mathbf{S}$ be an arbitrary, full-rank, matrix, such that $\mathbf{S}_k = \mathbf{S}\mathbf{D}_k$ is full rank, and let $\mathbf{X}_k = \mathbf{A}_{\boldsymbol{\Theta}}\mathbf{S}\mathbf{D}_k$ define a sequence of matrices. Then,* $\operatorname{span}(\mathcal{R}(\mathbf{X}_0)) = \operatorname{span}(\mathcal{R}(\mathbf{X}_k))$.

According to Proposition 2, starting with modulo measurements $\mathbf{Y}$, we can map them to the space spanned by the covariance of conventional samples $\mathbf{X}$. This is advantageous because existing methods can be readily applied. This results in the following recovery algorithm.

Recovery Algorithm

Inputs: Data matrix of modulo samples $\mathbf{Y}$ in (6).
Number of sources M.
An estimate on the upper bound, $\mathcal{B}_x \geq \|\{\mathbf{x}_l\}_{l=0}^{L-1}\|_{\mathbf{L}_\infty(\mathbb{R})}$.
Step 1: Compute K using (11).
Step 2: Compute $\mathbf{Z}$ using (16).
Step 3: Evaluate SVD, $\mathbf{Z} = \mathbf{U}\boldsymbol{\Sigma}\mathbf{V}^{\mathsf{H}}$ or $\mathcal{R}(\mathbf{Z}) = \mathbf{U}\boldsymbol{\Sigma}^2\mathbf{U}^{\mathsf{H}}$.
Step 4: Use traditional techniques for DoA estimation.
Output: $\boldsymbol{\Theta} = \{\theta_m\}_{m=0}^{M-1}$.

In the above recovery method, depending on the DoA estimation technique employed, specific constraints over the number of sources M, samples N and array elements L should be considered [1]. For example, for MUSIC and ESPRIT algorithms, the requirement is that $L > M$.

IV. Numerical Demonstration

In this section, we provide examples of DoA estimation. Furthermore, we consider the noisy case which shows that our approach is empirically stable in the presence of perturbations.

Noiseless Case We consider $M = 4$ transmitted, bandlimited signals $s_m \in \mathcal{B}_\pi$ which are randomly generated. We use $N = 8$ with $T = (2\pi e)^{-1} - 1/100$. The corresponding DoA angles $\{\theta_m\}_{m=0}^{3}$ are 3, 15, 45 and 87 degrees. We consider a ULA with $L = 11$ elements. Inter-element spacing is set to half a wavelength. Based on the experimental parameters, we construct the ground truth $\mathbf{X}$ and choosing $\lambda = 0.2$ we obtain $\mathbf{Y}$. A row of $\mathbf{X}$ and corresponding $\mathbf{Y}$ is shown in Fig. 2(a). The value of $\mathcal{B}_x$ is assumed to be known. With these parameters, we estimate K using (11). We perform the DoA estimation on $\mathbf{Z}$ in (16) and $\mathbf{X}$, using the MUSIC algorithm. As shown in Fig. 2(b) for a given row, $\mathbf{Z}$ is equal to $\mathbf{X}\mathbf{D}_K$. The MUSIC pseudo-spectrum is shown in Fig. 2(c). The results for $\mathbf{Z}$ and $\mathbf{X}$ are equal up to MATLAB's numerical precision.

Noisy Case Next, we evaluate our algorithm's performance in the case of noise. To this end, we consider the additive white Gaussian noise (AWGN) model. For comparison, we add noise to the conventional and modulo samples. As we do not use any denoising methods, this experiment serves as an empirical test of our algorithm's stability. We use the same experimental parameters as above, but with $N = 800$ and retrieve the DoAs using the ESPRIT algorithm with $M = 2$ (angles are 3 and 15 degrees). The SNR varies from 0 to 50 dB. The accuracy of the method is assessed using the MSE between the estimates and the ground truth. The experiment is averaged over 5000 trials for both noisy versions of $\mathbf{X}$ and $\mathbf{Y}$, respectively. The results are shown in Fig. 2(d). As expected, for low SNR, our method is unable to work with noisy measurements. Nonetheless, as the SNR increases, the method reaches a performance comparable to operating directly with the unfolded samples. The formal integration of noise into US-DoA is left for future research.

V. Conclusions

In this work, we presented a novel sensing approach for DoA estimation that is based on modulo non-linearity. Our work can tackle arbitrarily high-dynamic-range signals without running into the saturation problem. This is well suited for

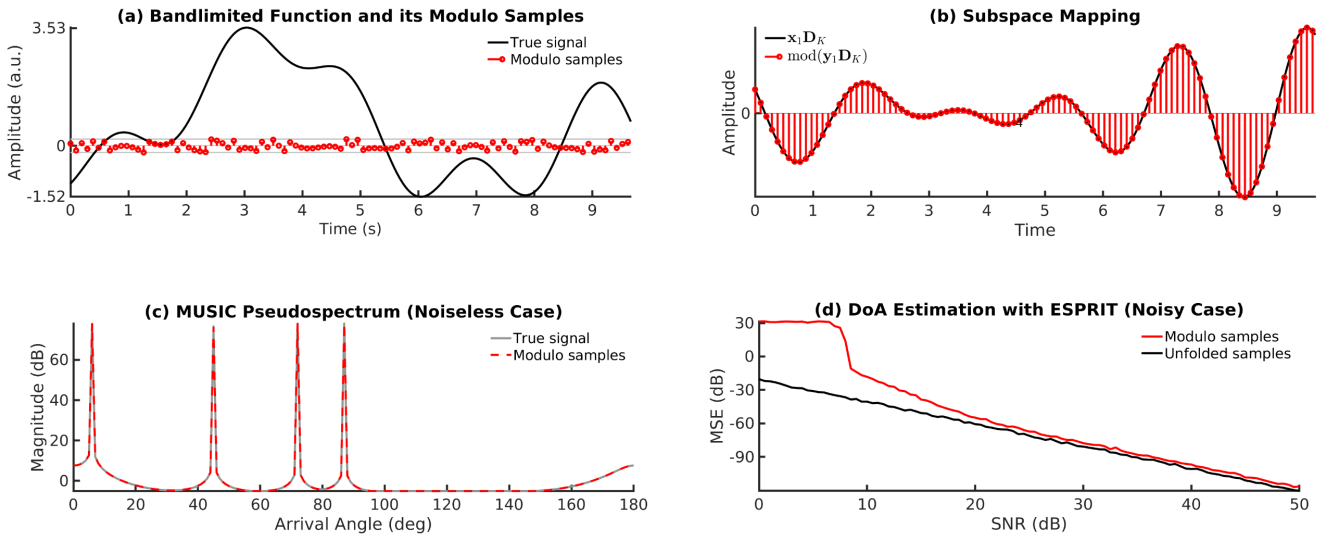

Fig. 2: (a) Bandlimited waveform, $x_1(t)$, and corresponding modulo samples $y_1[n]$, $\lambda = 0.2$ and $T = (2\pi e)^{-1} - 1/100$. (b) We show that $\mathbf{x}_1\mathbf{D}_K$ is the same as $\mathscr{M}_\lambda(\mathbf{y}_1\mathbf{D}_K)$ with K in (11). (c) MUSIC pseudo-spectrum using the covariance matrix of data $\mathbf{X}$ and $\mathscr{M}_\lambda(\mathbf{Y}\mathbf{D}_K)$. Both results are equivalent since our pre-processing operator retrieves the original signal subspace. (d) MSE between estimated and real DoA using ESPRIT algorithm, in terms of the SNR of the noise, using both $\mathbf{X}$ and $\mathscr{M}_\lambda(\mathbf{Y}\mathbf{D}_K)$. We can see that, in the low SNR regime, the pre-processing approach does not perform accurately since (11) does not hold for any value of K.

applications where ambient dynamic range is unknown or near field emitter/interferer may cause sensor saturation. The key advantages of our method are (a) non-iterative recovery, (b) backwards compatibility with known DoA estimation methods and (c) preservation of the original, unfolded signal. This allows for applications such as beamforming which is not possible with other alternatives such as the 1-bit architecture. Finally, our approach is based on a new kind of non-linear sensing setup, which leads to several interesting research questions on both the algorithmic and hardware fronts.

References

[1] T. E. Tuncer and B. Friedlander, Eds., *Classical and modern direction-of-arrival estimation*. Academic Press, 2009.

[2] H. Krim and M. Viberg, "Two decades of array signal processing research: The parametric approach," *IEEE Signal Process. Mag.*, vol. 13, no. 4, pp. 67–94, Jul. 1996.

[3] P. P. Vaidyanathan and P. Pal, "Sparse sensing with co-prime samplers and arrays," *IEEE Trans. Signal Process.*, vol. 59, no. 2, pp. 573–586, Feb. 2011.

[4] D. Romero, D. D. Ariananda, Z. Tian, and G. Leus, "Compressive covariance sensing: Structure-based compressive sensing beyond sparsity," *IEEE Signal Process. Mag.*, vol. 33, no. 1, pp. 78–93, 2015.

[5] P. Pal and P. P. Vaidyanathan, "Nested arrays: A novel approach to array processing with enhanced degrees of freedom," *IEEE Trans. Signal Process.*, vol. 58, no. 8, pp. 4167–4181, Aug. 2010.

[6] G. Tang, B. N. Bhaskar, P. Shah, and B. Recht, "Compressed sensing off the grid," *IEEE Trans. Inf. Theory*, vol. 59, no. 11, pp. 7465–7490, Nov. 2013.

[7] D. Malioutov, M. Cetin, and A. S. Willsky, "A sparse signal reconstruction perspective for source localization with sensor arrays," *IEEE Trans. Signal Process.*, vol. 53, no. 8, pp. 3010–3022, Aug 2005.

[8] A. Bhandari, F. Krahmer, and R. Raskar, "On unlimited sampling," in *12th Intl. Conf. on Sampling Theory and Applications (SampTA)*, Jul. 2017.

[9] ——, "On unlimited sampling and reconstruction," 2019, (preprint) arXiv:1905.03901.

[10] ——, "Methods and apparatus for modulo sampling and recovery," U.S. patent US10 651 865B2, May, 2020.

[11] J. Lai, Y. Xu, X. Zhang, and Z. Tang, "Structural analysis of lunar subsurface with Chang E-3 lunar penetrating radar," *Planetary and Space Science*, vol. 120, pp. 96–102, Jan. 2016.

[12] R. H. Dietz, D. E. Rhoades, and L. J. Davidson, "Apollo experience report–Lunar module communications system," National Aeronautics and Space Administration (NASA), techreport TN D-6974, Sep. 1972.

[13] R. Cao, S. Earp, S. A. L. de Ridder, A. Curtis, and E. Galetti, "Near-real-time near-surface 3D seismic velocity and uncertainty models by wavefield gradiometry and neural network inversion of ambient seismic noise," *GEOPHYSICS*, vol. 85, no. 1, pp. KS13–KS27, Nov. 2019.

[14] B. Wang, Y. Zhao, and J. Liu, "Mixed-order music algorithm for localization of far-field and near-field sources," *IEEE Signal Process. Lett.*, vol. 20, no. 4, pp. 311–314, Apr. 2013.

[15] B. Brannon, "Wideband radios need wide dynamic range converters," *Analog Dialogue*, vol. 29, no. 2, pp. 11–12, 1995.

[16] W. Oberhammer and B. Li, "Dynamic range extension of wideband receiver," U.S. patentus US6 333 707B1, 2001.

[17] O. Bar-Shalom and A. Weiss, "DOA estimation using one-bit quantized measurements," *IEEE Trans. Aerosp. Electron. Syst.*, vol. 38, no. 3, pp. 868–884, Jul. 2002.

[18] P. J. Soh, B. V. den Bergh, H. Xu, H. Aliakbarian, S. Farsi, P. Samal, G. A. E. Vandenbosch, D. M. M.-P. Schreurs, and B. K. J. C. Nauwelaers, "A smart wearable textile array system for biomedical telemetry applications," *IEEE Trans. Microw. Theory Techn.*, vol. 61, no. 5, pp. 2253–2261, may 2013.

[19] M. Allam and J. Greenleaf, "Isomorphism between pulsed-wave Doppler ultrasound and direction-of-arrival estimation. I. Basic principles," *IEEE Trans. Ultrason., Ferroelectr., Freq. Control*, vol. 43, no. 5, pp. 911–922, Sep. 1996.

[20] J. Rhee and Y. Joo, "Wide dynamic range CMOS image sensor with pixel level ADC," *Electron. Lett.*, vol. 39, no. 4, p. 360, 2003.

[21] S. Hirsch, M. Strobel, W. Klingler, J. D. S. Spüntrup, Z. Yu, and J. N. Burghartz, "Realization and opto-electronic characterization of linear self-reset pixel cells for a high dynamic CMOS image sensor," *Advances in Radio Science*, vol. 17, pp. 239–247, Sep. 2019.

[22] A. Bhandari, F. Krahmer, and R. Raskar, "Unlimited sampling of sparse sinusoidal mixtures," in *IEEE Intl. Sym. on Information Theory (ISIT)*, Jun. 2018.

[23] ——, "Unlimited sampling of sparse signals," in *IEEE Intl. Conf. on Acoustics, Speech and Sig. Proc. (ICASSP)*, Apr. 2018.